

# ADAPTIVE IMPEDANCE CONTROL FOR BILATERAL TELEOPERATION OF LONG REACH, FLEXIBLE MANIPULATORS

Lonnie J. Love and Wayne J. Book  
*The George Woodruff School of Mechanical Engineering  
Georgia Institute of Technology  
Atlanta, Ga. 30332-0405*

**Abstract:** Current applications in the field of telerobotics, such as space based assembly and nuclear waste remediation, require the use of long reach manipulators. These robots are characterized by their large workspace and reduced mass. Unfortunately, this reduction in mass increases structural compliance making these robots susceptible to vibration. Until recently, no attempt has been made to provide the operator any type of force reflection due to the compliance of the slave robot. This research addresses the control of bilateral teleoperation systems that use long reach flexible manipulators. Experiments indicate that the compliance of the slave robot directly affects the stability of the teleoperation system. Our study suggests that this may be controlled by increasing the damping on the master robot. This increase in target damping increases the effort an operator must exert during the execution of a task. To circumvent this limitation, the authors propose an adaptive impedance control paradigm. A new teleoperation strategy adapts the target impedance of the master robot to variations in the identified impedance of the remote environment coupled to the slave robot. Experiments suggest increased performance due to a decrease in the power the operator must provide during the execution of a task.

**Keywords:** Impedance control, Adaptive, Teleoperation, Robot Arm, Force control, Identification, Flexible arms

## 1. LONG REACH TELEOPERATION

Many teleoperation systems consist of a master and slave manipulator that are approximately the same sizes. New applications, such as micro manipulation and space based assembly require motion and force scaling between the master and slave robots (Colgate 1991). Figure 1 illustrates the teleoperation testbed used in this investigation. The system consists of a master robot scaled to human arm motion and a slave robot that has a workspace approximately fifty times the master robot's workspace. One potential application of such a system is the remediation of large nuclear waste storage facilities. In specifications for the nuclear waste restoration project, the operator may be located miles from the contamination site (Kreig 1990). Our testbed simulates this real world scenario and provides further insight into remote manipulation using long reach manipulators. To isolate the human operator from the slave environment, the master and slave robots are located in different labs in the same building. This configuration allows the investigators to control the visual, acoustic, and tactile cues that the operator experiences.

### 1.1 Slave Robot Workspace

The control of compliant manipulators has been a topic of active research for the past 20 years at Georgia Tech (Book 1993). The slave robot, RALF (Robotic Arm Long and Flexible), is a 2 DOF long reach manipulator that may be indicative of possible designs used in the nuclear waste restoration process. It consists of two cylindrical links with a span of 10 feet each and has a payload capacity of 60 lbs. while its link weight is only 100 lbs. (Huggins et al. 1987). A modular scaffold next to the slave robot permits simple

modifications to the slave robot's environment. This task board can be configured for tasks such as teleoperated pick-and-place, constrained manipulation, remote path following, and basic assembly such as the peg-in-the-hole insertion problem. The operator views the motion of RALF on two monitors that display black and white camera views of the slave robot's workspace. The first camera view, displayed on a 25" diagonal monitor, records a 20' x 15' vertical plane of motion from the side with a line of sight perpendicular to the robot's plane of motion. The second camera is mounted at the tip of the second link of RALF. This provides visual feedback of the robot's end-effector. A 9" diagonal monitor displays roughly a 14" x 10" rectangle in the plane of the end-effector.

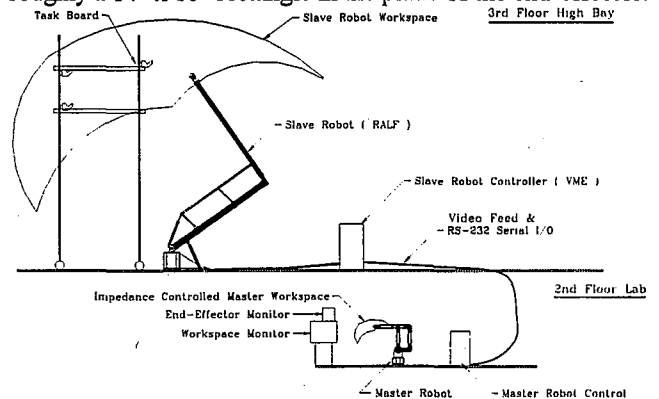


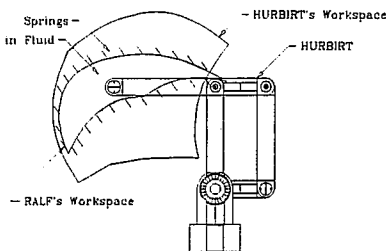
Figure 1: Long Reach Teleoperation Testbed

### 1.2 Master Robot

HURBIRT (Human Robot Bilateral Research Tool), a two degree of freedom haptic interface, serves as the master robot

for the teleoperation scheme (Love and Book 1994). To facilitate the teleoperation tasks, the controller for HURBIRT computes and scales its tip position from the space of the master robot to the space of the slave, RALF. Currently, a 7:1 position amplification permits comfortable mapping of RALF's full workspace into the workspace of the human operator. Once the desired tip position for RALF is calculated, the desired joint position vector is computed and then transmitted to the VME bus for input to the slave robot's controller. Currently, data is transmitted via a high speed serial communication port every 10 ms at 38,400 baud.

HURBIRT uses a computed torque impedance control algorithm. One example of the use of target impedance of the master robot is illustrated in Figure 2.



The workspaces of the master and slave manipulators in Figure 1 are dissimilar. Simple tasks such as moving the slave robot to its home position prove to be difficult by visual cues alone. The target impedance of the master robot, using the same philosophy of superimposing impedances described by Hogan (1985), is augmented with virtual walls that constrain the operator from commanding the slave robot outside its workspace. The target impedance for the robot is defined in (1).

$$M_t \ddot{x} + B_t \dot{x} + F_{vf} = F_h + \frac{1}{g} F_e \quad (1)$$

The target mass and damping matrices,  $M_t$  and  $B_t$  respectively, control the ease with which the operator moves the master robot based on the position of its tip,  $x$ . The two external stimuli to the master robot include the human applied force,  $F_h$ , and the interaction force between the slave robot and its environment,  $F_e$ . The scale,  $g$ , is the motion amplification between the master and slave robots. For proper bilateral force reflection, the slave force must be scaled by the inverse of this value. An additional virtual force,  $F_{vf}$  represents the repulsive force produced by deforming the virtual fixtures, in this case stiff walls constraining the effective workspace of the master robot. Four compliant spheres, mapped inside the master robot's workspace, replicate the limits of the slave robot's workspace. If the operator manipulates inside the scaled slave robot's workspace, the robot effectively "feels" like a mass moving through a viscous fluid. However, if the human attempts to command the robot outside its workspace, the virtual walls push the operator back into the workspace. Extensions of this example can include sophisticated forms of obstacle avoidance. While this is not a direct form of force reflection, the use of virtual fixtures provides a physical sensation of characteristics of the remote environment beyond the scope of direct force feedback. Equation (2) provides a

model of HURBIRT's dynamic equations of motion with respect to the generalized coordinates,  $q$ . This model includes the inertial matrix,  $D(q)$ , the gravitational load,  $\phi(q)$ , and the damping and nonlinear velocity terms. Forces applied to the robot include the joint torque,  $\tau$ , and the external force,  $F_e$ , projected to the generalized coordinates through the transpose of the Jacobian,  $J(q)$ .

$$D(q) \ddot{q} + C(q, \dot{q}) \dot{q} + \phi(q) = \tau + J^T(q) F_h \quad (2)$$

The control law in (3) provides the torque required to compensate for the robot's natural dynamics as well as provide the target impedance in (2).

$$\tau = D(q) J^{-1}(q) \left\{ M_t^{-1} \left[ F_h + \frac{1}{g} F_e - F_{vf} - B_t \dot{x}_m \right] - \ddot{J}(q) \dot{q} \right\} + C(\dot{q}, q) \dot{q} + \phi(q) - J^T(q) F_h \quad (3)$$

The following sections address how the selection of the target impedance affects not only the resistance the operator feels, but the stability of the teleoperation system.

### 1.3 Teleoperated Tasks

A vertical board, representing a wall in the remote environment, is attached to the task board in the slave robot's workspace. Markers on the wall indicate a path the operator is to follow during the execution of the teleoperated task. Furthermore, the operator is to attempt to maintain constant pressure on the wall while moving along this path. The operator begins the task by moving the slave robot from its home position to the top of the wall. After contact is established, the operator moves vertically down the surface of the wall while trying to maintain a constant contact force. After completing the path, the operator maneuvers the robot back to the home position. When the operator starts the task, he initializes the states measured during the execution of the task. These states include the task execution time, the power provided by the human to the master robot, and the net interaction force at the tip of the slave and master robot.

## 2. STABILITY OF BILATERAL TELEOPERATION

The problems associated with bilateral teleoperation of flexible manipulators reflect similar trends of problems described in bilateral teleoperation systems with time delays. The slave robot's mechanical compliance produces time delays in the form of wave propagation between the joint actuators and force sensor at the end of the robot. This produces an effective delay between an action generated by the human and the reaction force measured at the tip of the slave robot. A survey of bilateral teleoperation systems with time delays provides some explanation of the problems, and potential solutions to bilateral teleoperation of compliant manipulators.

Ferrel (1966) described stability limitations of bilateral teleoperation systems with transmission delays between the master and slave manipulators. Delays beyond 300ms potentially destabilize a bilateral teleoperation system. If

forces are fed back to the operator, who also provides the position command to the slave, they will tend to move the operator's hand. With excessive delays, the feedback is not only a source of information, but may act as a disturbance as well. This closed system, just as any closed loop system with long delays, can become uncontrollable. Systems with purely visual feedback can avoid instability by adopting a move and wait strategy. Unfortunately, this philosophy does not work well with tasks that require contact between the slave robot and its environment. Vertut et al. (1981) addresses stability and proposes limiting the velocities of the system and reducing the bandwidth to stabilize a bilateral teleoperation system with time delays. Hannaford and Anderson (1988) show through experimentation that additional damping at the master robot stabilizes teleoperation systems during collision with stiff environments. Operators reported that the system felt viscous and unresponsive. They suggest some form of on-line adaptation to adjust the damping of the master robot to the task.

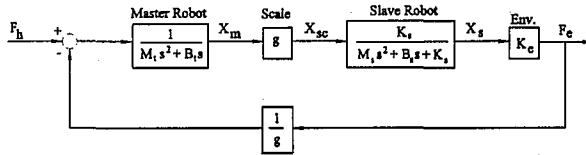


Figure 3: Teleoperation block diagram

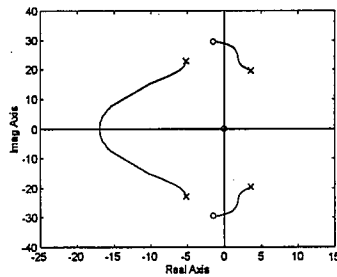


Figure 4: Locus of poles varying  $B_s$

Figure 3 illustrates a simplified block diagram of the teleoperation system. A flexible manipulator is a distributed parameter system that is theoretically infinite dimensional. Furthermore, the link compliance produces nonminimum phase zeros in the robot's transfer function between joint actuation and tip force sensors. For our stability analysis, we truncate the model of the flexible manipulator and only include the first mode of vibration. RALF's first natural frequency is 4.5 Hz and has a damping ratio of approximately 0.05. This is approximated by a second order system with a mass of 5.7kg, viscous damping of 17 N/m/s and stiffness of 5000N/m. The environment has a stiffness of approximately 2000 N/m. Furthermore, the master robot has a target mass of 10 kg. Figure 4 illustrates the locus of the system's closed loop poles as the target damping of the master robot increases from zero to infinity. This exercise is not intended to predict instability as much as illustrate trends in the systems stability

based upon the master robot's target impedance. Evidently, the stability of the teleoperation system can be controlled by adjusting the target damping of the master robot. Furthermore, as the environment stiffness increases, higher target damping of the master robot is required.

### 3. FIXED IMPEDANCE BILATERAL TELEOPERATION

The first method of bilateral teleoperation fixes the target impedance of the master robot. The target impedance of the master robot has high target damping to ensure limited oscillatory motion during contact with the environment. For this series of experiments, the target impedance in Eq. (1) has a 10 kg diagonal mass matrix with a 167 N/m/s diagonal damping matrix. Figure 5 illustrates the motion profile during the tenth iteration of the task described in Section 1.3. Figures 6 and 7 illustrate the interaction force between the slave robot and environment and the human applied force on the master robot during the tenth iteration of the task. The vibration measured at the tip of the slave robot propagates back to the master, evident in Figure 7. This low frequency vibration, approximately 1 Hz, is only evident during translation along the wall. After 20 repetitions of the task, the mean power provided by the human to the master robot is 148 N-m with a variance of 11.8 N-m. Likewise, the mean integrated force at the slave robot is 129.9 N-s with a variance of 8.9 N-s.

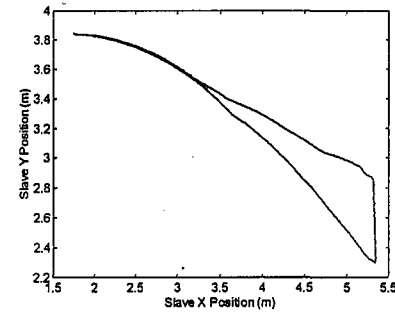


Figure 5: Slave Trajectory During Task

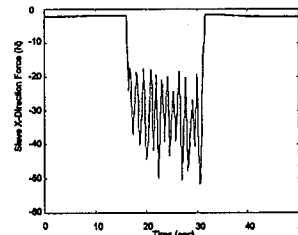


Figure 6: Slave Interaction Force,  $B_t=167$  N/m/s

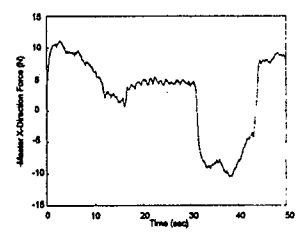


Figure 7: Human Force at Master,  $B_t=167$  N/m/s

The previous stability analysis suggests improper selection of master robot's target impedance can potentially drive the bilateral teleoperation system unstable. Figure 8 illustrates the motion response of the slave robot if the target damping is set to 20 N/m/s. The lower damping decreases the amount of energy required to move the master robot when the slave robot

is unconstrained. However, this also increases the sensitivity of the system to vibration, as illustrated in the force profiles in Figures 9 and 10.

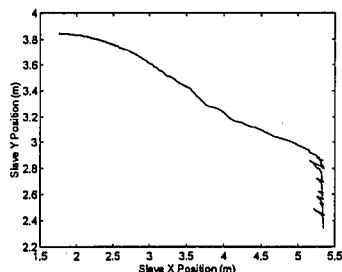


Figure 8: Slave Motion w/Bt=20N/m/s

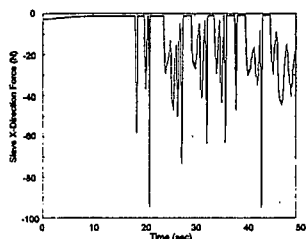


Figure 9: Slave Force, Bt=20N/m/s

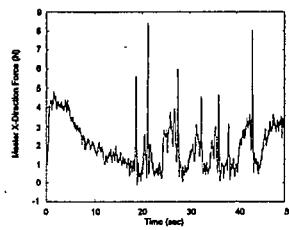


Figure 10: Master Force, Bt=20N/m/s

The lower target damping of the master robot reduces the effort the operator must apply to complete a task. However, the system may become unstable when the compliant slave robot interacts with a stiff environment. To ensure safe operation, the target damping of the master robot is increased. However, this increases the effort the operator must exert during the execution of the task. This provides the motivation for an adaptive impedance controller that adapts to variations in the slave's environment.

#### 4. REMOTE ENVIRONMENT ESTIMATION

To circumvent the limitations of fixed impedance control paradigms, adaptive impedance control of the master robot is considered. When the slave robot is unconstrained, the environmental stiffness is zero. Under this condition, the viscous resistance of the master robot should be light (Hannaford and Anderson 1988). However, when the slave robot approaches a constraint surface, the target damping on the master robot should increase to provide stable bilateral teleoperation.

Love and Book (1995) describe a method of identifying the dynamic characteristics of a robot's environment. One approach to modeling a position dependent representation of a robot's environment is to discretize the robot's workspace. Each of these discrete cells, illustrated in Figure 11, represents a small volume of the robot's workspace. The objective is to use these cells as position dependent storage units for the results of a recursive environment estimation process. A multi-input, multi-output, recursive least squares algorithm (MIMO-RLS), using tip force and position information,

estimates the dynamic characteristics of the robot's environment. After each cycle of the estimation process, the updated parameters of the environment model are averaged with previous results and stored in the cell that corresponds to the current tip position of the robot. To provide adequate resolution without excessive memory requirements, a 100x100 element array is used to model the slave robot's workspace. Each element of the two dimensional array corresponds to a seven centimeter square area of the slave robot's workspace.

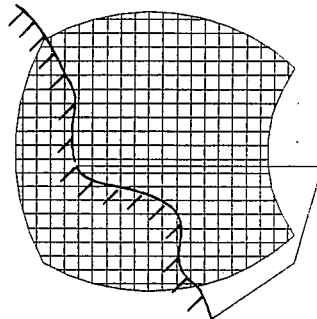


Figure 11: Quantized Workspace & Environment

Figure 12 illustrates the basic process executed each cycle of the estimation routine. The tip force and position vectors are measured and filtered through the RLS algorithm which provides an updated estimate of the environment mass, damping, and stiffness matrices. At the same time, the current tip position of the robot is correlated with a cell whose contents are extracted from memory. The parameters stored in the cell corresponding to the current tip position of the robot are updated with the latest estimate of the environment parameters. This provides a time varying position dependent model of the environment dynamics.

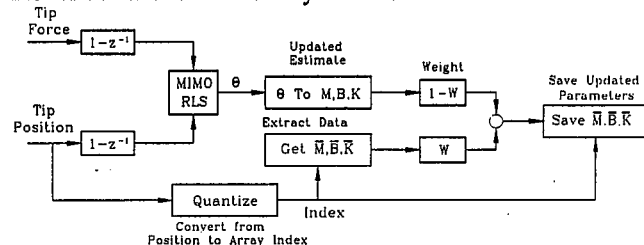


Figure 12: Flow Chart for Environment Estimation

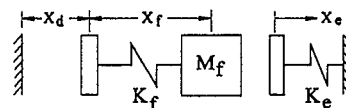


Figure 13: Flexible Robot contacting Environment

##### 4.1 Environment Estimation with a Flexible Robot

A fundamental assumption of the environment estimation is that the position of the end-effector is measurable. With a rigid manipulator, this is straightforward. However, static and dynamic deformation of the links on a compliant manipulator complicate this task. Figure 13 illustrates a simplified model of a 1-DOF elastic manipulator. The mass,  $M_f$ , and spring,  $K_f$ , represent the inertia and compliance of the elastic robot. Measurable states on the robot include the joint displacement,  $X_d$ , and tip force,  $F_e$ . The actual tip position,  $X_e$ , is equivalent to the sum of the rigid body displacement,  $X_d$  plus the deflection of the beam,  $X_f$ . If the system in Figure 13 is in

static equilibrium and the reference coordinate system is  $X_e$ , the interaction force between the robot and the constraint surface is expressed in Eq. (4).

$$\begin{aligned} F_e &= K_f X_f \\ &= -K_e (X_f + X_d) \end{aligned} \quad (4)$$

This produces a relationship between the tip deflection and the joint position, (5).

$$X_f = -\frac{K_e}{K_f + K_e} X_d \quad (5)$$

Equation (6) defines the relationship between the interaction force between the robot and environment,  $F_e$ , and the joint position,  $X_d$ .

$$F_e = -\frac{K_f K_e}{K_f + K_e} X_d \quad (6)$$

Thus, the relationship between the interaction force and the joint displacement is the stiffness of the robot and environment in series. This philosophy holds with the quasi static model of a multiple degree of freedom elastic manipulator.

## 5. REMOTELY ADAPTING IMPEDANCE CONTROL

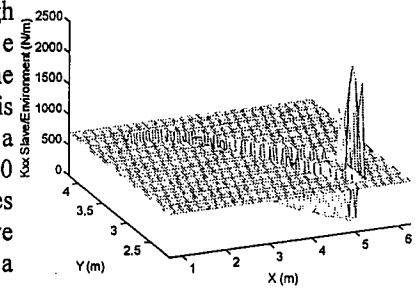
This section describes a new approach to adapting the target impedance of the master robot based upon an on-line estimation of the remote environment coupled to a flexible robot. The target impedance of the master robot adapts to variations in the identified impedance of a remote environment being operated on by a slave robot. The damping for the target impedance of the master robot is defined in (7).

$$B_t = 2 \zeta_t \sqrt{M_t K_e(x, y)} \quad (7)$$

High environment impedance is assumed when the operator maneuvers the slave robot into a region where high uncertainty exists in the environment estimation. As the robot maneuvers through this region, the environment estimation updates the model of the remote environment. As this estimate improves, the target impedance of the master robot adjusts appropriately. Consider the limiting case where the slave robot moves through unconstrained space. As the robot first moves through this space, the teleoperation system assumes the environment has a high stiffness value. This is accomplished by initializing the environment stiffness in each of the cells of Figure 11 to a high default value. If the robot is unconstrained, this stiffness gradually converges to zero, decreasing the target damping in this region. This target damping has a lower threshold of 10N/m/s.

During the execution of a task, an on-line estimation algorithm identifies the characteristics of objects in the slave robot's workspace. Figure 14 illustrates the resulting  $K_{xx}$  stiffness grid after 10 repetitions of the task. Evidently, there is a region of space in which the estimated environment stiffness is negligible. This region coincides with the unconstrained

space that the robot maneuvers through during the execution of the task. Each cell is initialized with a stiffness of 700 N/m. This ensures that when the slave robot moves into a new region, the adapted target



impedance is the same as the target impedance used in the fixed impedance bilateral teleoperation experiments with  $B_t = 167$  N/m/s. As the robot moves through unconstrained space, these cells converge to zero stiffness reducing the target damping of the master robot's impedance controller. Thus, the robot adapts its damping based upon the remote environment impedance. If the operator attempts to maneuver into a new region, the viscous resistance of the master robot increases in concert with the default high environmental stiffness values. Likewise, regions with identified high stiffness provide higher damping on the master robot.

The same series of experiments covered in Section 3 are conducted using the adaptive impedance control paradigm. After 20 repetitions of the task, the mean power provided by the human to the master robot is 59.6 N-m with a variance of 10.1 N-m. Likewise, the mean integrated force at the slave robot is 124.3 N-s with a variance of 7.9 N-s. The flexibility of the slave robot and environment is most evident in the force profiles recorded during the task. Figures 15 and 16 illustrate the external force due to the environment on the slave as well as the human applied force on the master. After the robot contacts the wall, a low frequency vibration is generated. Due to the force feedback to the master robot, the operator feels this vibration, but is capable of maintaining contact and completing the task.

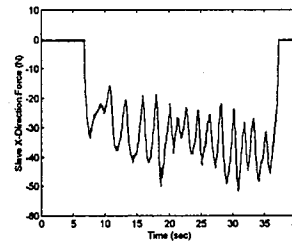


Figure 15: Slave Interaction Force

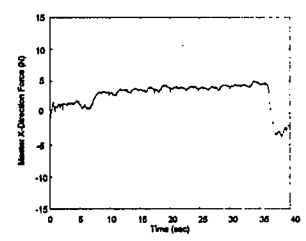
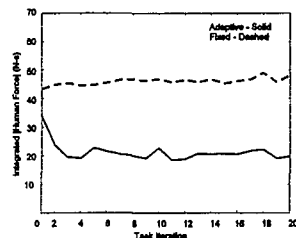


Figure 16: Human Force at Master

## 6. COMPARISON OF ADAPTIVE AND FIXED IMPEDANCE BILATERAL TELEOPERATION

A quantitative comparison of the two bilateral teleoperation systems provides insight into the potential for adaptive bilateral teleoperation systems. The only difference between the teleoperation experiments is the addition of the adaptive

damping based upon estimated environment impedance. The initial stiffness of 700 N/m ensures that the adaptive impedance controller has the same target impedance as the fixed impedance when the slave robot maneuvers into a new region. An operator executed the task twenty times, first using the adaptive teleoperation system. Next, the same operator executed the same task twenty times using the fixed impedance teleoperation scheme. Figure 17 illustrates the integrated force provided by the operator to the master robot during the execution of the task. This performance measures suggest that adapting the target impedance of the master robot, based upon an estimate of the environment impedance, improves the performance of the bilateral teleoperation system.



**Figure 17: Comparison of Human Applied Force**

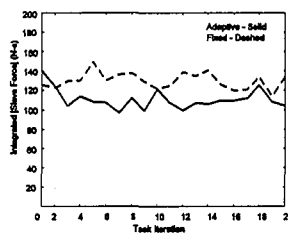


**Figure 18: Comparison of Slave Forces**

Figure 18 compares the integrated interaction force at the slave robot using fixed and adaptive impedance control on the master robot. Based on this display we see that, for both master arm controllers, the task is performed with approximately the same level of forces indicating comparable task performance. A comparison of Figures 17 and 18 suggests that less energy is required of the human to complete the same task. This reduction in energy reduces the potential for fatigue during repetitive teleoperated tasks.

## 7. CONCLUDING REMARKS

Impedance control provides a pragmatic approach to controlling the resistance of a robot coupled to a human. First, synthetic or virtual fixtures using potential fields provide a clear method of restricting the motion of a human during teleoperation. This research describes a novel approach to restricting the workspace of a master robot to the scaled workspace of a slave robot that contains a different workspace. One useful consequence of impedance control is the additive property of impedances. If the slave robot's workspace contains obstacles or restricted regions, additional potential fields can be added to the master robot's impedance controller. These potential fields provide resistance when the operator maneuvers the master robot towards these regions.

The versatility of impedance superposition is demonstrated through the described adaptive impedance control methods. A method for modeling and identifying a slave robot's environment is described. This model provides valuable information that improves the performance of bilateral teleoperation systems. One approach to adapting the target

impedance of the master robot is to control the damping ratio of the master robot. Adapting the target impedance to variations in the slave robot's environment can reduce the operator's energy, and thus reduce fatigue, during the execution of a task. During static contact experiments, no vibration is evident due to the flexibility of the slave robot. However, during contact hybrid force/motion tasks, a low frequency vibration is generated at the slave robot that propagates back to the operators. Future work will focus on vibration suppression techniques for the flexible robot and their role in bilateral teleoperation.

## ACKNOWLEDGMENTS

This research was sponsored in part by Sandia National Laboratories with the cooperation of Pacific Northwest Laboratories under contract No. 18-4379G.

## REFERENCES

- Book, W., 1993, "Controlled Motion in an Elastic World," *Journal of Dyn. Sys., Meas., and Control*, Vol. 115, No. 2B, p. 252-261.
- Colgate, E., 1991, "Power and Impedance Scaling in Bilateral Manipulation," *Proceedings, 1991 IEEE International Conference on Robotics and Automation*, pp. 2292-2297.
- Ferrell, W., 1966, "Delayed Force Feedback," *Human Factors*, pp. 449-455.
- Hannaford, B. and R. Anderson, 1988, "Experimental and Simulation Studies of Hard Contact in Force Reflecting Teleoperation," *Proceedings, 1988 IEEE Int. Conf. on Robotics and Auto.*, pp. 584-589.
- Hogan, N., 1985, "Impedance Control: An Approach to Manipulation: Part III - Applications," *ASME Journal of Dynamic Systems, Meas., and Control*, Vol. 107, pp. 17-24.
- Huggins, J., Kwon, D., Lee, J., Book, W., 1987, "Alternate Modeling and Verification Techniques for a Large Flexible Arm," *Proc, 1987 Conf. on Applied Motion Control*, pp. 157-164.
- Kreig, S., Jenkins, W., Leist, K., Squires, K., and Thompson, J., *Single-Shell Tank Waste Retrieval Study*, in *Westinghouse Hanford Co. Report for the U.S. Department of Energy*, 1990.
- Love, L., and Book, W., 1994, "Environment Estimation for Enhanced Impedance Control," *Proceedings, 1994 IEEE Int. Conf. on Robotics and Automation*, Nagoya, Japan, p. 1854-1859.
- Love, L. and W. Book, 1994, "Design and Control of a Multiple Degree of Freedom Haptic Interface," *Dynamic Systems and Control, 1994 ASME-WAM*, Chicago, IL, pp. 851-856.
- Vertut, J., Micaelli, A., Marchal, P., and Guittet, J., 1981, "Short Transmission Delay on a Force Reflective Bilateral Manipulator," *Proceeding, 4th Symposium. on Theory and Practice of Robotics and Manipulation*, pp. 269-285.